SSC22-VII-05

On-Orbit Characterization of a Microelectromechanical Systems (MEMS) Deformable Mirror (DM) on the Deformable Mirror Demonstration Mission (DeMi) CubeSat

Sophia K. Vlahakis
Department of Aeronautics and Astronautics, Massachusetts Institute of Technology
77 Massachusetts Ave, Cambridge MA 02139, USA; +1 617-253-7805
sophiakv@mit.edu

Faculty advisor: Professor Kerri Cahoy

ABSTRACT

The Deformable Mirror Demonstration Mission (DeMi) CubeSat operated from July 2020 to March 2022 and demonstrated the successful operation of a Microelectromechanical Systems (MEMS) Deformable Mirror (DM) on orbit for the first time. The payload design is an adaptive optics system with a 140-actuator MEMS DM from the Boston Micromachines Corporation (BMC) and a Shack-Hartmann wavefront sensor (SHWFS). DMs can correct wavefront errors from a variety of sources to improve image quality. MEMS DMs are particularly well suited for space systems because they are compact low power devices and have a high density of actuators with a large stroke to provide high precision wavefront control. This paper discusses on-orbit measurements characterizing the MEMS DM through analysis of deflections of individual actuators on the DM over time as they responded to input voltages up to 150 V, as measured by the on-board SHWFS. Repeatability is characterized by the differences between on-orbit actuator displacements commanded to the same voltages, which are shown to have a median of 2-13 nm. On-orbit DM actuation is shown to be similar to ground testing performance. The DeMi mission results have raised the Technology Readiness Level (TRL) of MEMS DM technology from a 5 to a 9.

INTRODUCTION

The Deformable Mirror Demonstration Mission (DeMi) satellite was a 6U CubeSat which successfully demonstrated the operation of a Microelectromechanical Systems (MEMS) Deformable Mirror (DM) on orbit for the first time. It was launched to the International Space Station (ISS) in February of 2020, was deployed into Low Earth Orbit in July of 2020, and finally deorbited at the end of its natural lifetime in March of 2022.

DMs function as part of adaptive optics systems by changing their shape to enhance the quality of images by correcting for wavefront errors due to thermal, optical, and mechanical effects. The applications of DM technology include astronomy, laser communications, space-situational awareness, re-configurable optics, and more.[1–4] One promising use of DMs and adaptive optics is for direct imaging of exoplanets, which requires high precision wavefront control in order to detect and characterize potentially habitable worlds in other solar systems.[5–7] MEMS DMs are well suited for space applications because they are compact devices which consume a small amount of power while having a high actuator density and large stroke to perform high precision wave-front control.[8–11] While MEMS DMs have been demonstrated on high altitude balloons[12,13] and sounding rockets,[14,15] the DeMi mission represents the first known successful operation of a MEMS DM in orbit, demonstrating their ability to survive rocket launch and operate in the radiation and thermal environment of space. The results of this mission have raised the Technology Readiness Level (TRL) of MEMS DM technology from a 5 to a 9.[16]

The DeMi payload design is a miniature space telescope equipped with adaptive optics technology including a 140-actuator MEMS DM from Boston Micromachines Corporation (BMC) and a Shack Hartmann wavefront sensor (SHWFS). The mission objectives included on-orbit characterization of the MEMS DM, on-orbit demonstration of closed-loop mirror control, and improvement of the point spread function (PSF) of an astronomical source. Specifically, the DeMi mission aimed to measure individual DM actuator wavefront displacement contributions to 12 nm precision, and to use active wavefront con-

trol to correct static and dynamic wavefront errors to less than 100 nm RMS error in space.

Payload Hardware Overview

The DeMi optical payload is shown in Fig. 1, reproduced with permission.[17] In addition to the MEMS DM, the payload design contains a 635 nm calibration laser source for internal observations, an image plane wavefront sensor to measure the system PSF, and a SHWFS to measure wavefront shape.[18] Further information on the DeMi mission development and payload design can be found in previous published works.[17–28] The experiments discussed in this paper characterize the DM by illuminating it with the internal laser and measuring the shape of the resulting wavefront with the SHWFS as the DM actuates.

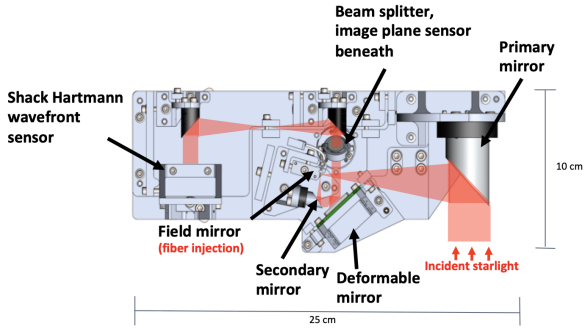

Figure 1: Diagram of the DeMi optical payload, reproduced with permission[17]

MEMS DMs are made out of polysilicon film layers etched to form actuators which are addressed individually through wire channels on a ceramic carrier.[29] To change the shape of the mirror, each actuator on the DM is sent an individual voltage command. The DM on board DeMi is a 140-actuator MEMS DM from BMC, with an actuator pitch of 450 μm and maximum actuator stroke of 5.5 μm.

The SHWFS is made up of an array of lenslets which focus incident collimated light into an array of spots on a CMOS detector in order to give information about the shape of the incident wavefront. When an actuator on the DM is deflected, the wavefront incident on the SHWFS will be distorted, causing the locations of the spots on the detector to be shifted. Through zonal reconstruction, the centroid displacements of the spots are used to reconstruct the wavefront shape, as discussed in subsection *"Actuator Poke Test Overview."*

During ground testing, both an interferometer and the SHWFS were used to measure the deflection of individual actuators on the DM. It was shown that the SHFWS is capable of measuring actuator deflection to within 10 nm of the interferometric measurements.[17,30,31]

Operations and Payload Data

The DeMi payload was designed, constructed, and tested at the Massachusetts Institute of Technology (MIT) and then integrated into a 6U spacecraft bus built by Blue Canyon Technologies (BCT). DeMi operated in space from July 2020 when it was deployed from the ISS until it deorbited in March 2022. Early operations consisted largely of establishing communications with two ground stations, confirming all parts of the spacecraft survived launch intact, and debugging operational procedures.[16,17]

There were two types of payload experiments conducted onboard the DeMi satellite. The first were actuator poke tests, which are the focus of this paper, and the second were wavefront control experiments, which use the DM to correct misalignments in the optical payload from thermal and mechanical effects in space. Successful wavefront control experiments are discussed in previous works[16] and additional results will be reported in future publications.

Actuator Poke Test Overview

Actuator poke tests performed throughout the DeMi mission enabled characterization of the performance of the MEMS DM in space. In an actuator poke test, the internal laser illuminates the DM and reflects the light to the SHWFS. Each actuator is deflected (or "poked") one-by-one with a command at a certain voltage. For each individually poked actuator, the resulting centroid displacements of the SHWFS spot field are measured and saved to be downlinked where they are used to calculate the deflection of the actuator. Zonal reconstruction is used to calculate the wavefront shape from the centroid displacements with the Southwell geometry using the Moore-Penrose pseudoinverse approach.[32,33] To do this, the wavefront vector is solved for in the following equation:

$$As = Dw \tag{1}$$

Here, the A matrix represents the averaging of the slope measurements sampled by the SHWFS, s is a vector of the centroid displacement measurements, and D is a matrix which represents the derivative of w, the wavefront vector. The pseudoinverse of D (represented as $D^{\dagger}$) is calculated to solve for the wavefront vector, w:

$$w = D^{\dagger}As^{T} \tag{2}$$

The deflection height of the actuator is equal to half the amplitude of the wavefront reconstruction due to the reflection of the wavefront off of the DM. To measure the actuator deflection height, a 2D Gaussian is fit to the wavefront reconstruction and the amplitude of this Gaussian is divided by two. The uncertainty associated with this deflection measurement is given by the standard deviation of the residual of the Gaussian fit (wavefront reconstruction minus Gaussian function), divided by two in order to be in units of DM surface shape.

These poke test measurements provide information on how each actuator responded to voltage commands throughout the mission as the satellite experienced the space environment. Preliminary on-orbit actuator poke test data has been reported in previous publications.[16,17]

This paper provides an in-depth analysis of the complete set of DeMi actuator poke test data data from on-orbit operations, including discussion of actuator measurement repeatability, comparison to ground testing data, and the impact of the on-orbit thermal environment on DM performance.

ON-ORBIT ACTUATION POKE RESULTS

During on-orbit actuator poke tests, each actuator was deflected one-by-one to a specified voltage, and SHWFS spot field centroid displacements were recorded. While there are 140 actuators on the DM, only some of them were fully illuminated by the internal laser and could be included in analysis. The laser is dimmer towards the edges of its beam pattern so deflection data from actuators near the edge had higher measurement uncertainty. Some data points were not included in analysis if not enough of the deflected area on the DM during an actuator poke was illuminated by the laser to obtain a reliable Gaussian fit.

Due to the imperfect nature of space communications, not every payload experiment data file reached the ground fully intact. Many files were missing chunks, so a combination of an automated pipeline and visual assessment was used to identify when data was too incomplete to be reconstructed. For every on-orbit poke test, only measurements from actuators fully illuminated by the laser and with intact spot field centroid displacement measurements are included in analysis. Some files were more complete than others, resulting in an average of 16 actuator deflection measurements per poke test which could be analyzed. The number of actuators analyzed per experiment does not reflect on the quality of actuator performance; Actuator measurements were not excluded from analysis due to performance, only due to incomplete data transmission or poor laser illumination.

Actuator poke tests were conducted for a range of input voltages up to 150 V. Table 1 below summarizes all 16 poke tests downlinked over the course of the DeMi mission. Listed for each experiment are the input voltages, experiment dates, median actuator deflection height, the standard deviation of deflections (to describe the spread of deflection amounts across different actuators), and the number of actuator measurements which could be included in analysis.

The on-orbit actuator deflection measurements are in strong agreement with the data provided by the DM manufacturer, as shown in Fig. 2. In this figure, each point represents the median measured deflection for a poke test from Table 1, error bars for each test represent the standard deviation of actuator measurements, and the solid line shows a quadratic fit to the measurement data. The data from the DM manufacturer was collected using a DM driver which was too large for a 6U CubeSat, so a miniature version was developed and used for DeMi operations, and it was shown to have a similar performance.[17,34]

In order to compare deflection data from the DM manufacturer to data collected during DeMi testing and space operations, an optical diffraction model was used to predict a measurement calibration factor of 0.9 which accounts for the angle of the DM in the payload design.[17,30] The results in Fig. 2 also confirm that the new DeMi driver design performs similarly to the BMC driver, and that it continued to perform well in the space environment.

On-orbit data also agrees well with expectations from ground testing which is discussed in section *"Comparison to Ground Testing"* and is illustrated in Fig. 5. The results in Fig. 2 and Table 1 also show strong precision across multiple trials for each poke test voltage – even for trials separated by several months of satellite operations. The DM was able to perform consistently and accurately throughout its lifetime with no evidence of measured actuators becoming stuck or unresponsive.

Individual Actuator Performance

Figure 2 and Table 1 show that the median deflection for actuators during poke tests are similar across trials of the same voltage. To further investigate the performance of individual actuators and quantify measurement repeatability, Fig. 3 shows the measured deflection for individual actuators across mul-

Table 1: Summary of on-orbit actuator deflection poke tests

Input Voltage [V]	Test Date	Median Measured Deflection [nm]	Deflection Standard Deviation [nm]	Number of Actuators Included in Analysis
30	6/10/2021	32	3	10
40	8/10/2021	54	5	17
60	6/2/2021	113	14	6
	6/3/2021	117	7	22
	6/5/2021	114	10	26
	2/9/2022	119	8	17
80	8/9/2021	224	10	7
	8/16/2021	218	10	20
100	8/1/2021	352	22	16
	10/5/2021	359	24	21
120	7/30/2021	537	27	11
140	7/27/2021	770	48	12
	10/3/2021	768	25	16
150	6/24/2021	917	36	12
	6/24/2021	914	39	21
	6/28/2021	925	34	20

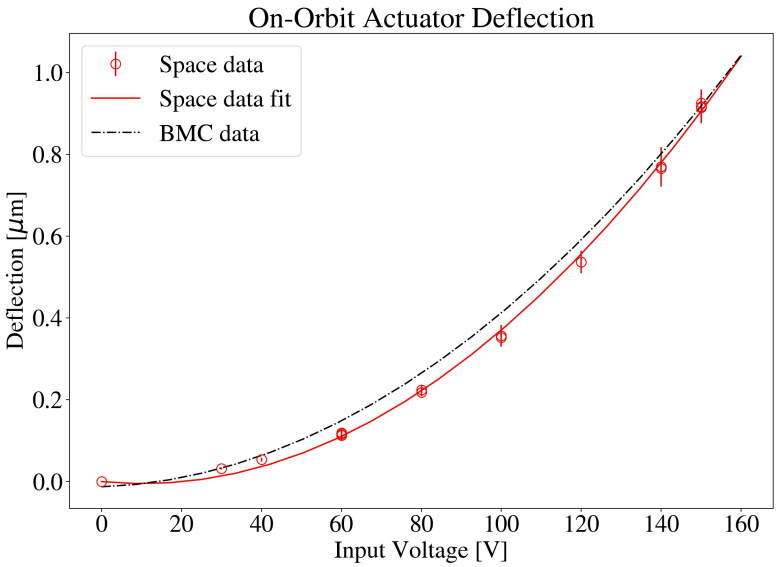

Figure 2: This figure depicts the measured actuator deflection on-orbit across a range of input voltages. Here, each point represents an on-board experiment described by a row in Table 1. This data shows good agreement between on-orbit actuator deflection measurements and data provided from BMC (the DM manufacturer). The manufacturer data plotted is multiplied by a calibration factor determined through optical modeling to account for the angle of the DM in the DeMi optical payload.[17,30]

tiple trials. Included in each of these plots are deflection values for any individual actuator pokes that were included in the analysis of more than one trial with the same voltage. The measurement uncertainties shown by the error bars in Fig. 3 are determined by the standard deviation of the residuals of the 2D Gaussian fits used to obtain the amplitude of the deflection from the wavefront reconstructions. The horizontal lines plotted show the median deflection for all actuators in a given trial (even those actuators which did not have repeated measurement).

The repeatability of deflection measurements for individual actuators is quantified in Table 2, which lists the median and maximum difference between measurements of the same actuators for each voltage. This table can only include voltage trials for which at least two experiments were conducted. The column "Median Deflection for Each Experiment" shows the median deflection across all actuators for each experiment at that voltage. It is important to note that due to incomplete data downlinks, the set of actuators analyzed is not the same across experiments, so the spread of these values is caused both by variance across actuators as well as the repeatability for individual actuators over time. The column "Median Difference in Deflection for Repeated Actuators" describes the median of the difference (maximum - minimum) in deflection for individual actuators which were included in the analysis of at least two of the experiments for a specified voltage. Since this value only compares deflection measurements of the repeated actuators, this column in Table 2 describes the repeatability of individual actuator performance.

As shown in Table 2, measurements of individual actuator deflections had a median difference of between 2-13 nm across different trials with the same voltage commands, demonstrating consistent repeatability over time. The standard deviation of deflection measurements across different actuators in a given poke test was between 3-48 nm (as seen in Table 1). The variation among measurements of the same actuators is smaller than the variation among the deflection of different actuators responding to the identical voltage commands across periods of time ranging from less than one day to nearly a year in space. This is illustrated in Fig. 3 by how data points for each actuator closely overlap even though there is variation in deflection across different actuators. This highlights the importance of calibrating the voltage response of each actuator individually, which will yield a greater precision than using an average response of all actuators.

COMPARISON TO GROUND TESTING

On the ground, actuator poke tests were conducted throughout the testing of the DeMi spacecraft. Measurements were taken in a thermal vacuum chamber at a temperature of approximately 6°C, and during several more tests between 24-29°C. Ground testing is discussed at length in previous work.[17,24,26,27] While the temperatures of the spacecraft payload were not recorded during on-orbit experiments, all experiments in space were completed during periods where the DeMi spacecraft was in eclipse. A histogram of recorded temperatures of the payload optics bench during eclipse periods is shown in Fig. 4. These eclipse temperatures have a mean value of 18°C and a standard deviation of 3°C.

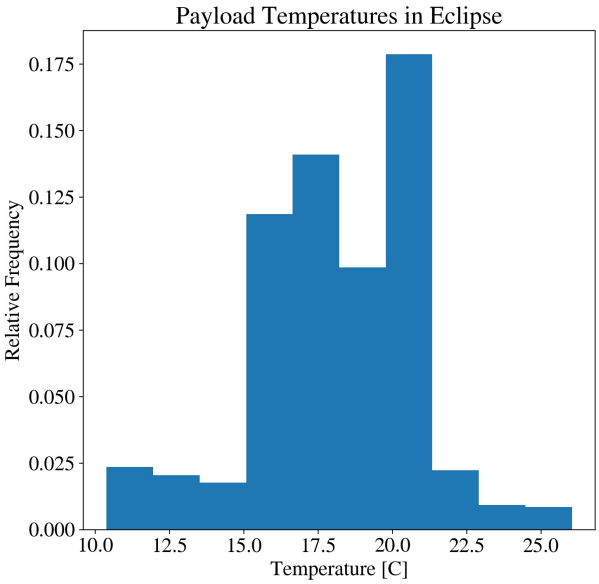

Figure 4: Measurements of on-board payload temperature from the DeMi satellite was in eclipse. The mean temperature from eclipse data is 18°C with a standard deviation of 3°C, which is used to estimate the temperature of on-board experiments.

The measured deflection with respect to input voltage for ground tests, manufacturer data, and space operations is plotted in Fig. 5. In this figure, error bars represent the the standard deviation of individual actuator deflection measurements and the trend lines display quadratic fits to the measurement data.

The deflection data for ground, space, and manufacturer tests all follow similar quadratic curves over the voltages tested. However, the deflection amount appears to vary across tests conducted at different temperatures, with smaller deflection amounts

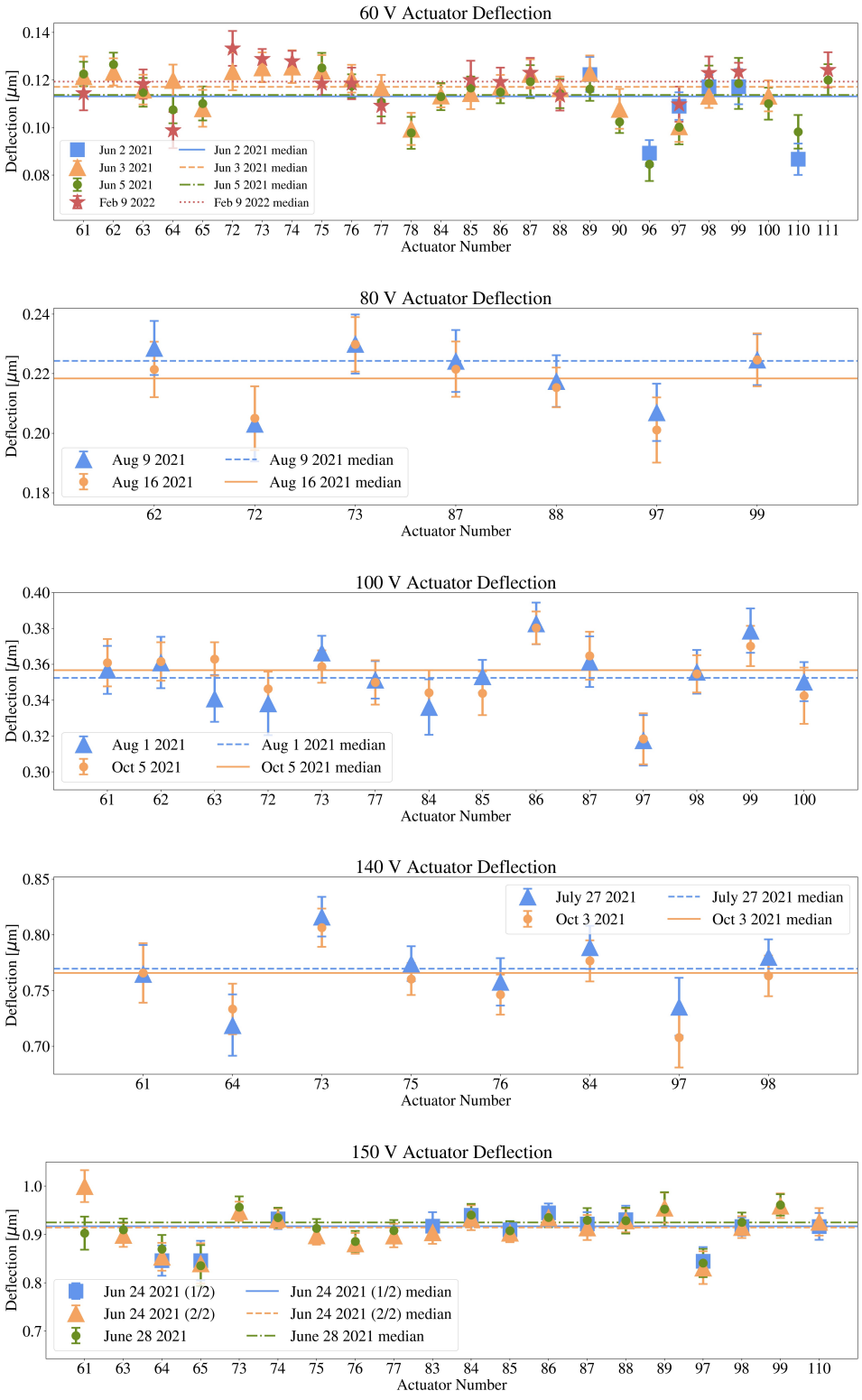

Figure 3: These plots illustrate the repeatability of on-orbit actuator deflection by comparing the measured deflection of individual actuators across experiments with the same input voltage. These measurements had a median difference of 2-13 nm, as described in Table 2. Note that the y-axis scales vary between these plots.

Table 2: Repeatability of on-orbit measurements of individual actuator deflection

Input Voltage [V]	Number of Experiments	Median Deflections for Each Experiment [nm]	Median Difference in Deflection for Repeated Actuators [nm]	Maximum Difference in Deflection for Repeated Actuators [nm]	Number of Actuators Compared
60	4	[113, 117, 114, 119]	5	21	26
80	2	[224, 218]	2	7	7
100	2	[352, 359]	6	22	14
140	2	[770, 768]	13	28	8
150	3	[917, 914, 925]	10	100	20

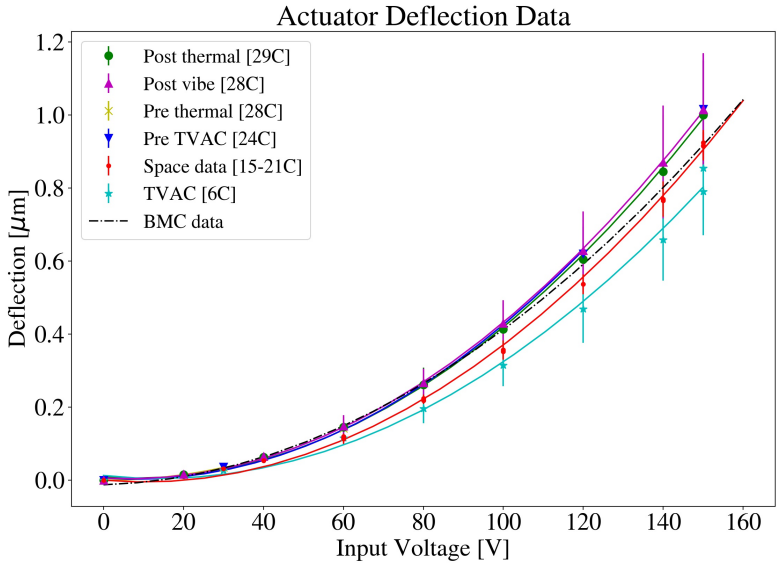

Figure 5: This figure shows the measured actuator deflection for ground tests, BMC manufacturer data (with a calibration factor), and on-orbit experiments. Solid lines are quadratic fits to data, and the temperature is listed in the legend for each set of trials. On-orbit data agrees well with ground testing and manufacturer data, with colder trials having slightly less deflection than warmer trials.

measured in colder temperatures. Through thermal modeling, the DeMi team has shown that thermal expansion and contraction in the SHWFS are insufficient to explain this trend, and testing from the manufacturer shows that the DM driver electronics should not have a strong thermal dependence. On average, actuators deflected 22% less at 6°C than at 28-29°C in the warmest trials. This difference in deflection reached 225 nm for inputs of 150 V.

The variation in deflection across different temperatures is further illustrated in Fig. 6, where actuator deflection amounts during poke tests are plotted against temperature for two example voltages: 30 V and 120 V. In this figure, the warmer ground experiments (24-29°C) are shown to have a higher median actuator deflection than the space data (18°C), which has a higher deflection than the coldest ground experiment (6°C). Within the warmest ground experiments between 24-29°C, the trend with temperature is not as clear, with the deflection decreasing a small amount for the very warmest 29°C experiment. Due to uncertainty in payload temperature recordings during these ground tests, it is unclear whether this decrease is a physical effect or due to temperature measurement error. Future experiments conducted at more temperatures and with greater precision in temperature measurement would help to quantify the relationship between temperature and actuator deflection amount.

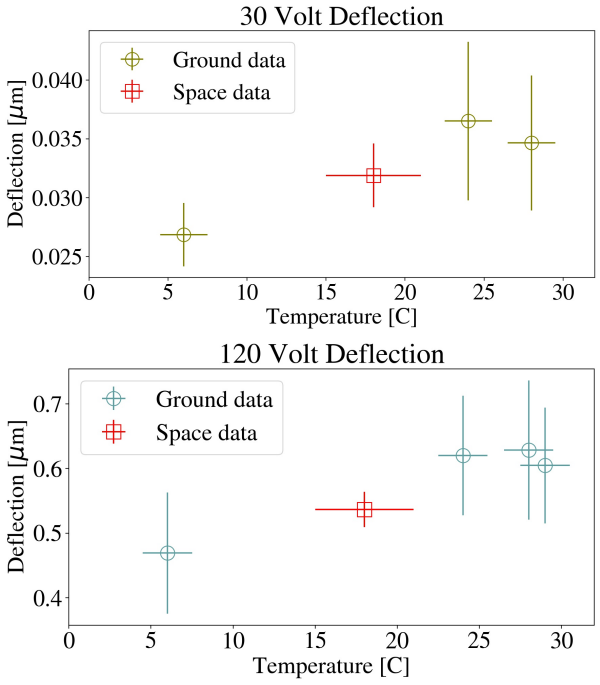

Figure 6: For ground and on-orbit experiments at 30 and 120 V, median deflection is shown to increase with temperature.

Previous cryogenic experiments in the literature using MEMS DMs from BMC have also documented decreases in actuator deflection at lower temperatures, likely due to thermal properties of the DM surface materials.[35] These cryogenic experiments also demonstrated that this temperature effect is more pronounced for higher spatial frequencies on the DM[35] – similar to the single actuator deflections in the DeMi actuator poke tests which are of high spatial frequency. The results of these cryogenic experiments align qualitatively with the temperature trend in actuator deflections present in Fig. 5. Future thermal modeling and experiments with BMC MEMS DM would further improve our quantitative understanding of the thermal effects these DMs experience in on-orbit thermal environments.

CONCLUSION

From July 2020 to March 2022, the DeMi CubeSat demonstrated the successful operation of a MEMS DM in space, raising the TRL of MEMS DMs to a 9.[16] Through experiments measuring the deflection of individual actuators on the DM using a SHWFS, the DM has demonstrated similar performance in space as on the ground. The optical payload survived launch intact and there was no evidence of actuators becoming stuck, unresponsive, or erratic during space operations. The repeatability in measured deflection for individual actuators on-orbit was shown to be 2-13 nm.

The DM deflected less at lower temperatures when evaluating tests conducted both in space and on the ground. The actuators deflected 22% less at 6°C in thermal vacuum chamber testing than in the warmest ground tests at 28-29°C. The on-orbit payload experiments are estimated to have been mostly between 15°and 21°C (as seen in Fig. 4), and the measured deflections in space are in between those of the colder and warmer ground trials, as shown in Fig 5. This dependence on temperature is likely due to thermal properties of the DM materials, and future modeling and testing may help to further characterize this relationship.

The success of the DeMi mission is a promising step towards the use of more DMs and adaptive optics systems in space for astronomy and other applications.[1–3] The use of DMs in space-based telescopes would help to correct wavefront error due to thermal and mechanical effects in space, and enable high precision wavefront control for high contrast imaging applications such as exoplanet direct imaging with coronagraphs to search for potentially habitable worlds around nearby stars.[5–7]

ACKNOWLEDGEMENTS

This research is based upon work supported by the Defense Advanced Research Projects Agency (DARPA) Program Office under Contract No. W31P4Q-16-C-0089. The DeMi bus was built by Blue Canyon Technologies and the mission was managed by Aurora Flight Sciences.

References

[1] Brendan Crill, Nick Siegler, Shawn Domagal-Goldman, Eric Mamajek, and Karl Stapelfeldt. Key Technology Challenges for the Study of Exoplanets and the Search for Habitable Worlds. Technical report, 2018. URL: https://arxiv.org/pdf/1803.04457.pdf.

[2] D. Grosse, F. Bennet, and M. Copeland et al. Adaptive optics for satellite imaging and earth based space debris maneuvers. In *Proc. 7th European Conference on Space Debris*, 2017.

[3] Craig Underwood, Sergio Pellegrino, Vaios Lappas, and et al. Using CubeSat/micro-satellite technology to demonstrate the Autonomous Assembly of a Reconfigurable Space Telescope (AAReST). *Acta Astronautica*, 114:112 – 122, 2015.

[4] Robert K. Tyson. *Principles of Adaptive Optics*. Academic Press, 1991.

[5] Wesley A Traub, Ben R Oppenheimer, and Sara (Ed.) Seager. Direct Imaging of Exoplanets. In *Exoplanets*, pages 111–156. 2010.

[6] B. R. Oppenheimer, C. Baranec, C. Beichman, D. Brenner, R. Burruss, E. Cady, J. R. Crepp, R. Dekany, R. Fergus, D. Hale, L. Hillenbrand, S. Hinkley, David W. Hogg, D. King, E. R. Ligon, T. Lockhart, R. Nilsson, I. R. Parry, L. Pueyo, E. Rice, J. E. Roberts, L. C. Roberts, M. Shao, A. Sivaramakrishnan, R. Soummer, T. Truong, G. Vasisht, A. Veicht, F. Vescelus, J. K. Wallace, C. Zhai, and N. Zimmerman. Reconnaissance of the hr 8799 exosolar system. I. near-infrared spectroscopy. *Astrophysical Journal*, 768(24), 2013.

[7] Sara Seager and Drake Deming. Exoplanet Atmospheres. *Annual Review of Astronomy and Astrophysics*, 48:631–672, 2010.

[8] Katie M. Morzinski, Julia W. Evans, Scott Severson, Bruce Macintosh, Daren Dillon, Don Gavel, Claire Max, and Dave Palmer. Characterizing the potential of MEMS deformable mirrors for astronomical adaptive optics. In *Proceedings of SPIE 6272 Advances in Adaptive Optics II*, 2006.

[9] Michael A. Helmbrecht, Min He, Carl J. Kempf, and Marc Besse. MEMS DM development at Iris AO, Inc. In *Proceedings of SPIE 7931 MEMS Adaptive Optics V*, 2011.

[10] Rachel Morgan, Ewan Douglas, Gregory Allan, Paul Bierden, Subriya Chakrabarti, Timothy Cook, Mark Egan, Gabor Furesz, Jennifer Gubner, Tyler Groff, Christian Haughwout, Bobby Holden, Christopher Mendillo, Mireille Ouellet, Paula do Vale Pereira, Abigail Stein, Simon Thibault, Xingtao Wu, Yeyuan Xin, and Kerri Cahoy. MEMS Deformable Mirrors for Space-Based High Contast Imaging. *Micromachines*, 366(10), 2019.

[11] Peter Ryan, Steven Cornelissen, Charlie Lam, Paul Bierden, and Thomas Bifano. Recent Progress in MEMS Deformable Mirrors, 2018.

[12] Timothy Cook, Kerri Cahoy, Supriya Chakrabarti, Ewan Douglas, Susanna C. Finn, Marc Kuchner, Nikole Lewis, Anne Marinan, Jason Martel, Dimitri Mawet, Benjamin Mazin, Mark Swain, Seth R. Meeker, Christopher Mendillo, David Stuchlik, and Gene Serabyn. Planetary Imaging Concept Testbed Using a Recoverable Experiment - Coronagraph (PICTURE C). *Journal of Astronomical Telescopes, Instruments, and Systems*, 1(4):044001, 2015.

[13] Olivier Côté, Guillaume Allain, Denis Brousseau, Marie-Pier Lord, Samy Ouahbi, Mireille Ouellet, Deven Patel, Simon Thibault, Cédric Vallée, Ruslan Belikov, Eduardo Bendek, Célia Blain, Collin Bradley, Olivier Daigle, Chris de Jong, David Doelman, René Doyon, Frédéric Grandmont, Michael Helmbrecht, Matthew Kenworthy, David Lafrenière, Frank Marchis, Christian Marois, Steeve Montminy, Frans Snik, Gautam Vasisht, Jean-Pierre Véran, and Philippe Vincent. A precursor mission to high contrast imaging balloon system. In Christopher J. Evans, Luc Simard, and Hideki Takami, editors, *Ground-based and Airborne Instrumentation for Astronomy VII*, volume 10702, pages 1306 – 1313. International Society for Optics and Photonics, SPIE, 2018.

[14] Ewan S. Douglas, Christopher B. Mendillo, Timothy A. Cook, Kerri L. Cahoy, and Supriya Chakrabarti. Wavefront sensing in space: flight demonstration II of the PICTURE sounding rocket payload. *Journal of Astronomical Telescopes, Instruments, and Systems*, 4(1):1 – 10, 2018.

[15] Christopher B. Mendillo, Brian A. Hicks, Timothy A. Cook, Thomas G. Bifano, David A. Content, Benjamin F. Lane, B. Martin Levine, Douglas Rabin, Shanti R. Rao, Rocco Samuele, Edouard Schmidtlin, Michael Shao, J. Kent Wallace, and Supriya Chakrabarti. PICTURE: a sounding rocket experiment for direct imaging of an extrasolar planetary environment. In *Proceedings of SPIE 8442 Optical, Infrared, and Millimeter Wave*, 2012.

[16] Rachel Morgan, Sophia K. Vlahakis, Greg Allan, Paula do Vale Pereira, Jennifer Gubner, Christian Haughwout, Bobby Holden, Thomas Murphy, Yinzi Xin, Kerri L. Cahoy, Ewan S. Douglas, John Merk, Danilo Roascio, Mark Egan, and Gábor Furész. Operations update for the deformable mirror demonstration mission (demi) cubesat. In *The Advanced Maui Optical and Space Surveillance Technologies Conference*, 2021.

[17] Rachel E. Morgan, Ewan S. Douglas, Gregory Allan, Paula do Vale Pereira, Jennifer N. Gubner, Christian Haughwout, Christian Haughwout, Thomas Murphy, John Merk, Mark D. Egan, Gábor Furész, Danilo Roascio, Yinzi Xin, and Kerri L. Cahoy. Optical calibration and first light for the deformable mirror demonstration mission CubeSat (DeMi). *Journal of Astronomical Telescopes, Instruments, and Systems*, 7(2):1 – 20, 2021.

[18] Ewan S. Douglas, Greg Allan, Rachel Morgan, Bobby G. Holden, Jennifer Gubner, Christian Haughwout, Paula do Vale Pereira, Yinzi Xin, John Merk, and Kerri L. Cahoy. Small mirrors for small satellites: Design of the deformable mirror demonstration mission cubesat (demi) payload. *Frontiers in Astronomy and Space Sciences*, 8:126, 2021.

[19] Kerri L. Cahoy, Anne D. Marinan, Benjamin Novak, Caitlin Kerr, Tam Nguyen, Matthew Webber, Grant Falkenburg, and Andrew Barg. Wavefront control in space with MEMS deformable mirrors for exoplanet direct imaging. *Journal of Micro/Nanolithography, MEMS, and MOEMS*, 13(1), 2014.

[20] Anne Marinan and Kerri Cahoy. CubeSat Deformable Mirror Demonstration. In *International Symposium on Optomechatronic Technologies*, 2014.

[21] Anne Marinan, Kerri Cahoy, John Merck, Ruslan Belikov, and Eduardo Bendek. Improving Nanosatellite Imaging with Adaptive Optics. In *Proceedings of AIAA/USU Conference on Small Satellites*, 2016.

[22] Ewan S. Douglas, Gregory Allan, Derek Barnes, Joseph S. Figura, Christian A. Haughwout, Jennifer N. Gubner, Alex A. Knoedler, Sarah LeClair, Thomas J. Murphy, Nikolaos Skouloudis, John Merck, Roedolph A. Opperman, and Kerri L. Cahoy. Design of the deformable mirror demonstration CubeSat (DeMi). In *Proceedings of SPIE 10400 Techniques and Instrumentation for Detection of Exoplanets*, 2017.

[23] Ewan S. Douglas, Gregory Allan, Derek Barnes, Joseph S. Figura, Christian A. Haughwout, Jennifer N. Gubner, Alex A. Knoedler, Sarah LeClair, Thomas J. Murphy, Nikolaos Skouloudis, John Merck, Roedolph A. Opperman, and Kerri Cahoy. Design of the deformable mirror demonstration CubeSat (DeMi). In *Proceedings of SPIE 10400 Techniques and Instrumentation for Detection of Exoplanets*, 2017.

[24] Jennifer Gubner. Payload Configuration , Integration and Testing of the Deformable Mirror Demonstration Mission (DeMi) CubeSat. In *32nd Annual AIAA/USU Conference on Small Satellites*, 2018.

[25] Jennifer Gubner. Deformable Mirror Demonstration Mission. B. S. thesis, 2018. URL: https://repository.wellesley.edu/ thesis-collection/606.

[26] Gregory Allan, Ewan S. Douglas, Derek Barnes, Mark Egan, Gabor Furesz, Warren Grunwald, Jennifer Gubner, Bobby G. Holden, Christian Haughwout, Paula do Vale Pereira, Abigail J. Stein, and Kerri L. Cahoy. The deformable mirror demonstration mission (DeMi) CubeSat: optomechanical design validation and laboratory calibration. 1069857(August 2018):180, 2018.

[27] Paula do Vale Pereira, B Holden, R Morgan, and et. al. Thermomechanical design and testing of the Deformable Mirror Demonstration

Mission (DeMi) CubeSat. In *Proceedings of the 2020 AIAA/USU Conference on Small Satellites*, 2020.

[28] Jennifer Gubner. The Deformable Mirror Demonstration Mission (DeMi) On-Orbit Analysis. Master's thesis, 2021.

[29] Thomas Bifano. Adaptive imaging mems deformable mirrors. *Nature Photonics*, 5(1):21–23, 2011.

[30] Rachel Morgan. Optical Modeling, Alignment, and Testing for the Deformable Mirror Demonstration Mission (DeMi) CubeSat Payload. In *34th Annual AIAA/USU Conference on Small Satellites*, 2020.

[31] Rachel Morgan. Optical modeling and validation for the Deformable Mirror Demonstration Mission. Master's thesis, 2020. URL: https://dspace.mit.edu/handle/1721.1/128059.

[32] W.H. Southwell. Wave-front estimation from wave-front slope measurements. *J. Opt. Soc. Am.*, 70(8):998–1006, Aug 1980.

[33] Guang-ming Dai. *Wavefront Optics for Vision Correction*. SPIE, 2008.

[34] Christian Haughwout. Electronics Development for the Deformable Mirror Demonstration Mission (DeMi). Master's thesis, 2018. URL: https://dspace.mit.edu/handle/1721.1/120438.

[35] Aoi Takahashi, Keigo Enya, Kanae Haze, Hirokazu Kataza, Takayuki Kotani, Hideo Matsuhara, Tomohiro Kamiya, Tomoyasu Yamamuro, Paul Bierden, Steven Cornelissen, Charlie Lam, and Michael Feinberg. Laboratory demonstration of a cryogenic deformable mirror for wavefront correction of space-borne infrared telescopes. *Applied Optics*, 56(23):6694–6708, 2017.